From Nuclear Waste to Hydrogen Production: From Past Consequences to Future Prospect

Johan Vandenborre, Simon Guillonneau, Guillaume Blain, Ferid Haddad, Laurent Truche

From Nuclear Waste to Hydrogen Production:

From Past Consequences to Future Prospect

1 *Johan VANDENBORRE[1*], Simon GUILLONNEAU[1,2], Guillaume BLAIN[1], Ferid HADDAD[3],*

4 *Laurent TRUCHE[2].*

5 [1]CNRS/IN2P3, Nantes Université, IMT Atlantique, SUBATECH, F-44000 Nantes, France

6 [2]University Grenoble Alpes, CNRS, ISTerre, CS 40700, 38058 Grenoble, France

7 [3]GIP ARRONAX, 1 rue ARRONAX, CS 10112, 44817 Saint-Herblain Cedex, France

8 **GRAPHICAL ABSTRACT:**
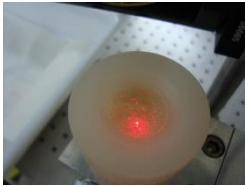
10 H_2 bubbles produced by the effect of radioactivity onto water (credit: Guillaume Blain in

11 ARRONAX, 2016)

12 **ABSTRACT:**

13 Nuclear wastes may not be considered as unusable materials in the sense that they deliver a free

14 source of energy under the form of ionizing radiations that can be used to produce hydrogen (H_2)

15 through water radiolysis. The current paradigm that define these nuclear wastes as troublesome

16 by-products which no one uses nowadays must be shifted into a new opportunity for pure H_2

17 production with no CO_2 emission. Here, we propose a low-tech method to boost H_2 production

18 by water radiolysis thanks to the catalytic effect of a suspension of TiO_2 nano-particles. We also

* Corresponding Author : johan.vandenborre@subatech.in2p3.fr

19   demonstrate the relevance of this concept by scaling up our laboratory results. From our

20   calculations, this radiocatalytic process can supply until 60% of the actual global demand in

21   hydrogen (42.9 $MtH_2.y^{-1}$) and open the door, together with the green and white hydrogen

22   productions, to the "Hydrogen century".

23   **KEYWORDS:** Nuclear Waste, Hydrogen Production, Radiocatalysis, TiO_2, LowTech Process

24

25   **1. Introduction**

26   To meet the net zero emission scenario of the International Energy Agency, about 300 Mt of

27   hydrogen-based energy has to be produced worldwide by 2050. Currently, water electrolysis

28   using renewable [1; 2] and nuclear electricity [3; 4] is the main industrial process envisioned to

29   produce large amount of hydrogen with low carbon emissions. However, beyond electricity

30   itself, many valuable resources like metals and land space will be consumed by this technology

31   scenario. Until now, water radiolysis, as a serious alternative to produced massive amount of H_2,

32   has been ignored. This radiolytic process of hydrogen generation is known for a century [5; 6],

33   but the nuclear energy industry still prefers to envision the use of its electricity (from the so-

34   called warm generator) to produced indirectly H_2 [3; 4], than taking advantage of the radiation

35   delivered by the spent fuel. Water radiolysis occurring naturally in the Earth's crust is known to

36   be a significant source of H_2 and to support deep microbial ecosystems [6; 7]. So much efforts

37   have been made to manage nuclear wastes that one has forgotten that they offer a free source of

38   radiations available all around the world. There is 390.000 tons of spent fuel worldwide awaiting

39   their final storage facilities (Data for 2017 [8]), and many more to come in a near future as

40   nuclear electricity is seen as good mean to mitigate CO_2 emissions.

41   **2. Material and Methods**

42   Four sets of samples are irradiated under Ar atmosphere to avoid the dioxygen effect: UltraPure

43   water (UP), UltraPure water and ZrO_2 (UP+ZrO_2), UltraPure water and TiO_2 anatase

44   (UP+TiO_2anat), UltraPure water and TiO_2 rutile (UP+TiO_2rutile). Ultrapure water resistivity was

45   measured at 18 MΩ.cm. All solid samples were purchased from Sigma-Aldrich (99.9% Purity)

46   and added to the solution with a ratio of 12.5 $g.L^{-1}$. The solution density is calculated at 1.052

47      $g.cm^{-3}$.

48   **2.1 Irradiation source**

49   γ-Ray irradiations experiments were performed at the ARRONAX cyclotron (Nantes – France)

50   facility. The irradiation cells were made of PEEK (polyether ether ketone), mounted with a

51   rotulex 19/9 glass tube and had an internal volume of 42 mL. The irradiation time range is

52   between 1 to 60 days. γ-Ray irradiation was performed with a GSM D1 (Gamma-Service

53   Medical[®]) irradiator containing a 123 TBq ^{137}Cs source. This radionuclide disintegrates in [137]Ba,

54   which delivers 661.7 keV γ-Ray. A dose cartography has been performed by Fricke dosimetry

55   [9] inside the γ-Ray chamber. The average deposited dose rate inside the aqueous samples is 420

56      $Gy.h^{-1}$. Such a modest dose rate has to be compared to the 28 $kGy.h^{-1}$ delivered by high activity

57   long life spent fuel. As γ-Ray is a penetrating radiation, the dose is displayed almost equally

58   everywhere inside the sample.

59

60   **2.2 Gas Measurements**

61   Hydrogen (H_2) has been monitored by micro gas-chromatography (µGC) using a 490-GC

62   (VARIAN[®]) micro gas-chromatograph. A 5 Å molecular sieve column dedicated to H_2

63   separation was used, coupled to a TCD detector. The injection system and the column were

64 purged with argon beforehand. All our chromatographic measurement were repeated 3 times,

65 with a precision of 3 % at the 95 % confidence level.

66   **2.3 Radiolytic yield calculation (G-value)**

67 The G-value is defined as the number of species formed or consumed per unit of deposited

68 energy. It is the main parameter used to express the production of one chemical species via the

69 radiolysis mechanism. It is expressed in the international system by mol.J^{-1} and is calculated at a

70 time t after transition of the ionizing irradiation according to:

71      $$G(X) = \frac{X_t}{\rho\,D} \qquad (1)$$

72   where X_t is the concentration of the species X at the time t (mol.L^{-1}), ρ is the density of the

73 irradiated solution (kg.L^{-1}) and D the absorbed dose (in Gy; 1 Gy = 1 J.kg^{-1} of water).
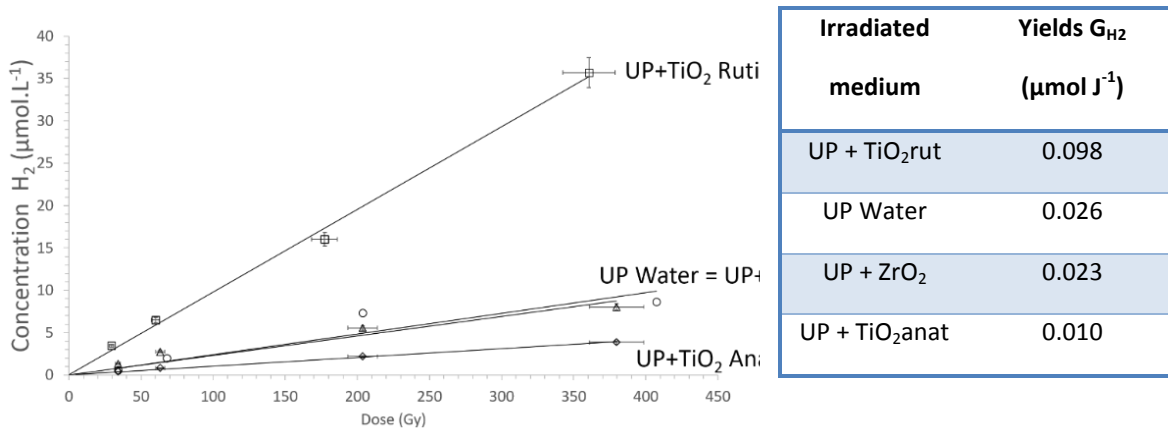
74

75

76 **Results**
77 Liquid water is exposed to a γ source (Cs^{137}) in order to mimic the γ-ray from the radioactive

78 waste. Hydrogen production is precisely measured for each irradiation time and applied dose

79 rate. Titanium dioxide rutile or anatase phase powders, chosen for its photocatalytic effect [10-

80 18], are added to the solution. Tetravalent oxide (zirconium) is also tested to underline the

81 specific surface properties of TiO_2 with respect to H_2 generation [16; 17; 19-23].

82 **Figure 1** presents the evolution of the radiolytic production of H_2 as a function of the applied

83 dose, which is itself a function of time as the dose rate of the γ-source is constant. From these

84 results one can easily observe that rutile-bearing experiment produced 4 times more H_2 than all

85 the other ones whether they contain only water, or another polytype of TiO_2 or ZrO_2. To our

86 knowledge, this is the highest H_2 yield measured so far in pure water solution.

87　　This enhanced production of H_2 is specific to the TiO_2 rutile which confirms its radiocatalytic

88　　properties. Interestingly, a parallel can be made with its photocatalytic properties. Indeed, it is

89　　well described in the literature [10; 15; 18] that in the presence of UV-Visible solar radiation the

90　　TiO_2 surface in contact with water solution promote the formation of $H°$, $OH°$, $O_2°^-$ and $HO_2°$

91　　radicals, i.e. the same species involved in the water radiolysis mechanisms [6]. Moreover, in

92　　photocatalytic experiment, TiO_2 rutile was already identified as a scavenger of the $OH°$ radical to

93　　enhance H_2 production on the contrary to ZrO_2 [17].

Irradiated medium	Yields G_{H2} ($\mu mol\ J^{-1}$)
UP + TiO_2rut	0.098
UP Water	0.026
UP + ZrO_2	0.023
UP + TiO_2anat	0.010

95　　**Figure 1.** Hydrogen production vs. dose, i.e. vs. the contact time between solution and γ -ray

96

97　　The **Equation (1)**, (SI) is established with specific parameters which must be taken into account

98　　for an industrial H_2 radiolytic production as follow:

99　　　　$$m_{H2} = G_{H2} \times \rho\ D_R \times T \times V_{sol} \times M \qquad (2)$$

100　　where m_{H2} is the dihydrogen production (in g), ρ is the density of the irradiated solution (1.05

101　　$kg.L^{-1}$, in the case of the TiO_2 rutile suspension), D the absorbed dose (in Gy, corresponding to

102　　the product of Dose Rate D_R of the γ -source in $Gy.h^{-1}$ and the contact time t in h), V_{sol} the

103　　irradiated volume of the solution (in L), G_{H2} is the H_2 radiolytic yield ($mol.J^{-1}$) and M the molar

104　　weight of H_2 (2.016 $g.mol^{-1}$).

5

105   From the G-value determined for the TiO_2 rutile system (0.1 $\mu mol.J^{-1}$) and **Equation (1)**, one can

106   upscale the H_2 production derived from our experiment lab conditions to realistic industrial

107   process. Here, we envision to circulate an aqueous suspension of TiO_2 rutile around a vitrified

108   high-level radioactive waste (Figure 2A). The water circulation circuits is connected to a

109   degasser in order to retrieve H_2 produced by water radiolysis. The HL Radwaste size is

110   considered as 135x44 cm with a mass of 500 kg and a dose rate $D_R = 14$ $kGy.h^{-1}$. These results

111   are calculated for two options with a different thickness of the water layer around the waste:

112   either 2 cm ($V_{sol} = 46$ L), either 10 cm ($V_{sol} = 294$ L) which corresponds to the average

113   penetration depth of the Cs γ-radiation.

114

115
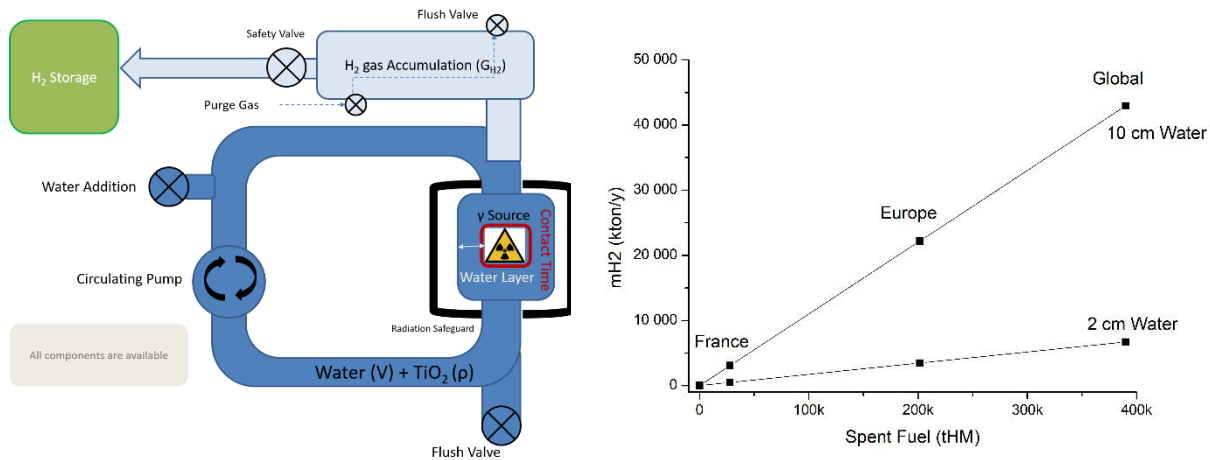
116

117

118   **Figure 2.** *A* : Scheme of H_2 production unit where the high level nuclear waste is surrounded
119   by a water container connected to a recirculation circuit and a degaser to recover H_2. The
120   thickness of the water layer surrounding the waste package should be around 2 to 10 cm to
121   maximize the effect of the γ-radiation penetration. *B* : Total H_2 radiolytic production via nuclear
122   waste inventory vs data sheet from AIEA [8] (Data inventory at 31th December 2016) with 10
123   and 2 cm for the water layer thickness around the waste.

124

125   The following important comments can be made from this calculation (see Eq. 2):

126   • G_{H2} : From our lab results we have used the 0.1 $\mu mol.J^{-1}$ value, but many yield
127   improvement can be proposed by scavenging processes which, for example, consumes
128   hydroxyl radical and enhances the H_2 production [24; 25].

129   • ρ : The density of pure water is 1 $kg.L^{-1}$, but one must take into account the density of the
130   aqueous suspension of TiO_2 rutile (1.05 $kg.L^{-1}$). This TiO_2 quantity could be optimized to
131   enhance the yield of H_2 production.

132   • γ Source: In our experimental lab we have used a classical ^{137}Cs source (Dose Rate = 420
133       $Gy.h^{-1}$) which is the main γ source emitting in the spent fuel for the first part of
134   radioactive decay (30 years). That is the reason why, from an industrial point of view, the
135   more efficient radioactive source is the High Activity-Long Life spent fuel actually
136   storage in different power plant (390 ktons) with an average dose rate calculated from
137   literature data [26] to 28 $kGy.h^{-1}$ per ton. So we can extend the actual experiment to the
138   spent fuel due to the same source term (^{137}Cs) in both cases with a difference between the
139   dose rate (28 vs. 0.420 $kGy.h^{-1}$).

140   • Contact Time: This time is the duration when the volume of solution is under the effect of
141   the irradiation. In this study, we have performed experiments lasting up to 2 months and
142   confirmed that the H_2 production occurs continuously with the TiO_2 surface scavenging
143   the $OH°$ species without poisoning [17]. Such a phenomenon does not happen with
144   ultrapure water only as the Allen chain stops the H_2 production process [6]. Thus, we
145   have chosen to calculate the H_2 production over one year to compare with other industrial
146   processes.

7

147   • Molar Weight: We have expressed the H_2 production in term of mass to compare with

148   other H_2 production methods already used.

149   • Volume of the solution (V): It is the key point for the H_2 radiolytic production. The H_2O

150   concentration (55.5 mol.L^{-1}) exposed to the radiation kinetically forces the H_2 production.

151   That is the reason why higher is the irradiated volume, higher is the H_2 production. The

152   H_2 radiolytic production kinetic occurs at μs scale [6]. Therefore, for both cases (2 and 10

153   cm water layer corresponding to the average penetration depth of γ-ray), we have

154   calculated the water flow rate accounting for the waste package geometry (46 and 294

155   L.s^{-1}, respectively).

156   • Production of H_2: For the 2 and 10 cm water layer, the production of radiolytic H_2 is

157   respectively 6.7 and 42.9 MtH_2 per year if we used the totality of spent fuel actually

158   stored in the world (value in 2017). This H_2 production can further be enhanced,   as

159   underlined in previous occurrences, by optimizing the irradiated solution volume, G_{H2}-

160   value, TiO_2/water ratio and water composition.

161

162   **3. Discussion: Consequences for low-carbon Hydrogen production**

163   From the hydrogen industry side, the global quantity of pure H_2 calculated in **Figure 2** (6.7 and

164   42.9 MtH_2.y^{-1}) represents about 10 and 60 % of the actual global H_2 production (70 MtH_2.y^{-1},

165   with only 0.6 MtH_2.y^{-1} being supplied as "green hydrogen" from renewable energy sources in

166   2019 [2]). Moreover, the so-called "green hydrogen" need high quantity of low-carbon

167   electricity, metals such as Cu, Co, Ni or Li and pure water to be relevant. In the radiolytic

168   production, the system proposed here can be considered as "low tech" due to : (i) a very modest

169   electricity need (just to circulate solution and not to initiate electrolysis), (ii) only Titanium

170   required as metal oxide native form and it is considered as the ninth more abundant element in

171   the earth's crust [27], (iii) many kind of water can be used (wastewater, seawater for example)

172   and (iv) all materials needed are commercially available without rare or strategic metals being

173   involved. Nevertheless, research and development on irradiated solution volume, G_{H2}-value,

174   TiO_2/water ratio and water composition remains to be carried out to enhance the global

175   production H_2 yield of the radiolytic process.

176

177   **4. Conclusion and Perspectives**

178   In this work, a new paradigm is proposed: spent nuclear fuel may not be seen as useless waste

179   but as a new unused free-carbon energy source via the H_2 radiolytic production by a lowtech

180   process. This system displays many advantages in addition to the classical "green hydrogen"

181   ones:

182   • The nuclear production energy is a decarbonized one, so the wastes produced via this

183   technology too.

184   • The long-live radioactivity delivered by nuclear waste allows to use it for many centuries

185   (> 300 years) with a low technology process.

186   • All spent nuclear fuel wastes produced from the start of the nuclear industry in 50's can

187   be used by this process (in 2017, 390 ktons).

188   • By the revival of the nuclear industry in the world (at least two-fold more in 2050), more

189   and more unused nuclear wastes will be available for this H_2 production process.

190   • At the contrary to the "green hydrogen" process which proposes to convert electricity in

191   hydrogen, which could be used for other decarbonized sectors, and reconvert it to

192   electricity with loss of yield; the radiolytic process proposes to convert unused nuclear

193   waste in electricity via the hydrogen production.

194   • Calculations from our experiments yield an H_2 production ranging give between 6.7 and

195   42.9 $MtH_2.y^{-1}$, depending on the water layer thickness considered around the waste. Its

196   represents between 10 to 60 % of the global demand in hydrogen and at least 10-fold the

197   present day actual production of "green hydrogen".

198   However, many parameters remain to be optimized to improve the H_2 production yield. These

199   parameters are as follow: irradiated solution volume, initial G_{H2}-value, TiO_2/water ratio and

200   water composition in order to accommodate the results presented here to the industrial realities.

201

202

203

208
209   REFERENCES

210   [1].   Lagadec, M.F., Grimaud, A., 2020. Water electrolysers with closed and open
211   electrochemical systems. Nature Materials 19, 1140-1150.

212   [2].   IEA, 2019. The Future of Hydrogen. IEA Paris, France, Report Prepared by the IEA for
213   the G20, Japan.

214   [3].   El-Emam, R.S., Dincer, I., 2017. Nuclear-Assisted Hydrogen Production, in: Meyers,
215   R.A. (Ed.), Encyclopedia of Sustainability Science and Technology. Springer New York, New
216   York, NY, pp. 1-11.

217 [4].   Constantin, A., 2024. Nuclear hydrogen projects to support clean energy transition:
218 Updates on international initiatives and IAEA activities. International Journal of Hydrogen
219 Energy 54, 768-779.

220 [5].   Giesel, F., 1902. Ueber radium und radioactive Stoffe. Berichte der deutschen
221 chemischen Gesellschaft 35, 3608-3611.

222 [6].   Allen, A.O., 1961. The Radiation Chemistry of Water and Aqueous Solutions, Princeton,
223 USA.

224 [7].   Lin, L.-H., Hall, J., Lippmann-Pipke, J., Ward, J.A., Sherwood Lollar, B., DeFlaun, M.,
225 Rothmel, R., Moser, D., Gihring, T.M., Mislowack, B., Onstott, T.C., 2005. Radiolytic H2 in
226 continental crust: Nuclear power for deep subsurface microbial communities. Geochemistry,
227 Geophysics, Geosystems 6.

228 [8].   IAEA, 2018. Status and Trends in Spent Fuel and Radioactive Waste Management.
229 International Atomic Energy Agency.

230 [9].   Fricke, H., Hart, E.J., 1966. Chemical Dosimetry, Radiation Dosimetry. Academic Press,
231 New York, USA.

232 [10].   Bai, S., Liu, H., Sun, J., Tian, Y., Chen, S., Song, J., Luo, R., Li, D., Chen, A., Liu, C.-C.,
233 2015. Improvement of TiO2 photocatalytic properties under visible light by WO3/TiO2 and
234 MoO3/TiO2 composites. Applied Surface Science 338, 61-68.

235 [11].   Ibrahim, N.S., Leaw, W.L., Mohamad, D., Alias, S.H., Nur, H., 2020. A critical review of
236 metal-doped TiO2 and its structure–physical properties–photocatalytic activity relationship in
237 hydrogen production. International Journal of Hydrogen Energy 45, 28553-28565.

238 [12].   Bzdon, S., Góralski, J., Maniukiewicz, W., Perkowski, J., Rogowski, J., Szadkowska-
239 Nicze, M., 2012. Radiation-induced synthesis of Fe-doped TiO2: Characterization and catalytic
240 properties. Radiation Physics and Chemistry 81, 322-330.

241 [13].   Takata, T., Jiang, J., Sakata, Y., Nakabayashi, M., Shibata, N., Nandal, V., Seki, K.,
242 Hisatomi, T., Domen, K., 2020. Photocatalytic water splitting with a quantum efficiency of
243 almost unity. Nature 581, 411-414.

244 [14].   Komaguchi, K., Nakano, H., Araki, A., Harima, Y., 2006. Photoinduced electron transfer
245 from anatase to rutile in partially reduced TiO_2 (P-25) nanoparticles: An ESR study. Chemical
246 Physics Letters 428, 338-342.

247 [15].   Escobedo, S., Rusinque, B., de Lasa, H., 2019. Photochemical Thermodynamic
248 Efficiency Factors (PTEFs) for Hydrogen Production Using Different TiO2 Photocatalysts.
249 Industrial & Engineering Chemistry Research 58, 22225-22235.

250 [16].   Yamada, R., Nagaishi, R., Hatano, Y., Yoshida, Z., 2008. Hydrogen production in the γ-
251 radiolysis of aqueous sulfuric acid solutions containing Al_2O_3, SiO_2, TiO_2 or ZrO_2 fine particles.
252 International Journal of Hydrogen Energy 33, 929-936.

253 [17]. Klett, C., Cui, Y., Devineau, S., Foy, E., Dagnelie, R., Renault, J.P., 2013. H_2 production
254 through oxide irradiation: Comparison of gamma rays and vacuum ultraviolet excitation.
255 International Journal of Hydrogen Energy 38, 3889-3897.

256 [18]. Liu, R., Wu, L., Liu, H., Zhang, Y., Ma, J., Jiang, C., Duan, T., 2021. High-Efficiency
257 Photocatalytic Degradation of Tannic Acid Using TiO2 Heterojunction Catalysts. ACS omega 6,
258 28538-28547.

259 [19]. Petrik, N.G., Alexandrov, A.B., Vall, A.I., 2001. Interfacial Energy Transfer during
260 Gamma Radiolysis of Water on the Surface of ZrO_2 and Some Other Oxides. J. Phys. Chem. B
261 105, 5935-5944.

262 [20]. Roth, O., Dahlgren, B., LaVerne, J.A., 2012. Radiolysis of Water on ZrO_2 Nanoparticles.
263 J. Phys. Chem. C 116, 17619-17624.

264 [21]. LaVerne, J.A., Tandon, L., 2002. H_2 Production in the Radiolysis of Water on CeO_2 and
265 ZrO_2. J. Phys. Chem. B 106, 380-386.

266 [22]. Cecal, A., Goanta, M., Palamaru, M., Stoicescu, T., Popa, K., Paraschivescu, A., Anita,
267 V., 2001. Use of some oxides in radiolytical decomposition of water. Radiation Physics and
268 Chemistry 62, 333-336.

269 [23]. Imanova, G., 2022. Molecular hydrogen production by radiolysis of water on the surface
270 of nano-ZrO2 under the influence of gamma rays. Synthesis and Sintering 2, 9-13.

271 [24]. Crumière, F., Vandenborre, J., Essehli, R., Blain, G., Barbet, J., Fattahi, M., 2013. LET
272 Effects on the Hydrogen Production induced by the Radiolysis of pure Water. Radiation Physics
273 and Chemistry 82, 74-79.

274 [25]. LaVerne, J.A., Ryan, M.R., Mu, T., 2009. Hydrogen production in the radiolysis of
275 bromide solutions. Radiation Physics and Chemistry 78, 1148-1152.

276 [26]. 2009. Classification of Radioactive Waste. INTERNATIONAL ATOMIC ENERGY
277 AGENCY, Vienna.

278 [27]. Emsley, J., 2011. Nature's building blocks: an AZ guide to the elements. Oxford
279 University Press.

280